OLIVINE ABUNDANCE ASSESSMENT USING THE RATIO OF 1- AND 2-μm INTEGRATED BAND DEPTHS: APPLICATIONS TO CHANDRAYAAN-1 M³ DATA. Y. Surkov[1], Y. Shkuratov[1], V. Kaydash[1], G. Videen[2], V. Korokhin[1], S. Velichko[1]; [1]Institute of Astronomy, V. N. Karazin Kharkiv National Univ., 35 Sumska St., Kharkiv, 61022, Ukraine, [2]Space Science Institute, 4750 Walnut St. Suite 205, Boulder CO 80301, USA.

Introduction: Olivine is a mineral considered as a component of the lunar mantle [1]. Many olivine-rich sites have been identified on the Moon according to data of Earth-based telescopic spectral observations [2-4] as well as multiband imagers onboard Clementine [5-6], Kaguya [7], and Chandrayaan-1 [8] spacecraft. The main source of olivine on the lunar surface probably is mantle material penetrating through the lunar crust by volcanism and large-scale impact events. However, the full set of mechanisms of surface mantle-formations is still unclear [9]. Insights regarding olivine presence in the regolith may be useful for further development of views on the lunar interior and surface-rock formation.

We propose a technique to assess the olivine abundance using M^3 Chandrayaan-1 data. It is focused on the modeling of spectral olivine indices [10]. We believe that such spectral parameters are stable enough to overcome data and calibrations shortcomings. In addition, they may be more specific to certain mineral component than reflectance values at several spectral channels. One of the most simple and common spectral indices of olivine is the ratio of integrated band depths of 1 and 2 μm absorption bands in lunar spectra [8,11]. We performed estimates of olivine abundance in the crater Copernicus (see Fig. 1).

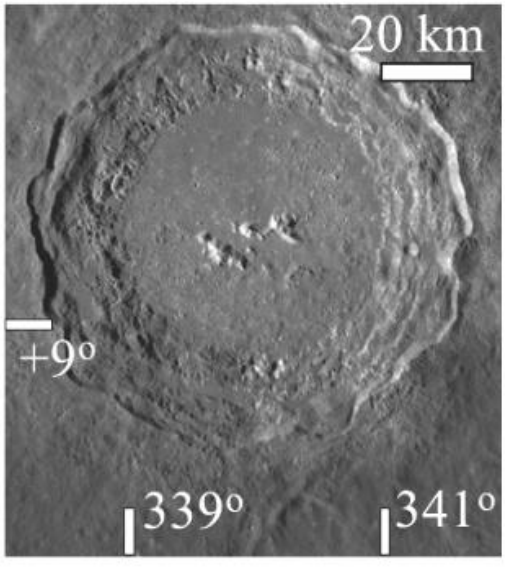

Figure 1. An albedo map of the crater Copernicus taken from: quickmap.lroc.asu.edu

Three regions rich in olivine have earlier been found in Copernicus: the peaks, small olivine-rich material deposits on the crater floor, and low albedo spots and flows on the northern wall [9]. This crater is very attractive for testing remote-sensing techniques, because of its mineral diversity and wide range of local illumination conditions and surface structure types. Pyroclastic deposits are another material, where the 1 μm band is wider than those typical of pyroxenes, and this band's minimum is shifted to 1.1 μm, and hence, spectrally similar olivine abundance may erroneously be estimated [12]. However, there are other signs allowing one to distinguish these cases.

Olivine abundance assessment procedure: we develop a spectral-mixing model [13] to construct a dataset of 1,000,000 synthetic spectra. These spectra represent spectral mixtures of the 5 main minerals of the lunar regolith: plagioclase (PLG), pyroxenes (PYR), olivine (OLV), ilmenite (ILM) and agglutinates (AGL). All mineral components were taken in some proportions.

The structure parameters of the model include the free path of light in particles (15 μm) and the regolith volume fraction occupied by particles (0.5). Refractive indices of minerals are n_{PLG} = 1.55; n_{PYR} = 1.6; n_{OLV} = 1.65; n_{ILM} = 2; n_{AGL} = 2. We use the spectra from the LRMCC dataset [14] for the fine fractions of PLG – LRCMP210_15058; PYR – LRCMP213_15555; OLV – LRCMP212_15555; ILM – LRCMP218_70017. The spectrum of AGL is LS-CMP-045 from the RELAB database. We use the spectra of the complex refractive index of Fe^0 from [15] to take into account changes in the spectral behavior of minerals due to space weathering, primarily due to $npFe^0$ granules formation. The volume fraction of $npFe^0$ was distributed from 10^{-4} to $5{\cdot}10^{-4}$. This procedure was not applied to plagioclase and agglutinates fractions. We study the correlation diagram of the Integrated Band Depths (IBDs) ratio vs. the olivine content measured in percent volume. This dependence is almost linear with a correlation coefficient of approximately 0.94; whereas, for other minerals it is significantly lower.

The volume concentration of olivine depends nonlinearly on the IBD ratio, which may be expressed by the following equation:

$$c_{OLV}\left[vol.\%\right] = 34.5\ln\left(IBD_1 / IBD_2\right) - 14 \quad (1)$$

We note that Eq. (1) has no physical sense if $IBD_1/IBD_2 < 1.5$. This can occur when the 1 μm absorption band is completely absent or is significantly dominated by the 2 μm band. This is a spectral indicator of olivine depletion. The nonlinearity may be cause under- or overestimation of olivine in mixtures with extremely high olivine content, where $IBD_2 \rightarrow 0$.

Results and discussion: We used portion of M^3 hyperspectral image M3G20090610T030313 for crater Copernicus. The image was initially processed as described in [16, 17] to reduce the M^3 artifacts.

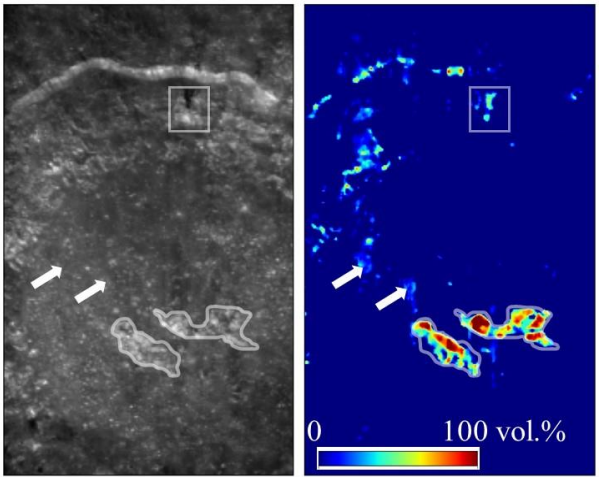

Figure 2 The M^3 albedo *A*(750 nm) (left) and olivine abundance maps of the crater Copernicus.

A map of the olivine content distribution of crater Copernicus shown in Fig. 2 reveals several regions of surface olivine exposures: (1) both contoured peaks; (2) the dark spot (in rectangle) and in flow-like structures to the west on the northern wall; (3) the floor deposits marked with arrows. This shows consistence with the data of Dhingra et al. [9]. All olivine locations are well localized and the average olivine content outside them is close to zero. The proposed technique is insensitive to other mineral components present on the crater floor, mainly plagioclase and pyroxenes.

The peaks are the most olivine abundant areas in this scene. The content of the mineral varies from 40 to 100 vol.%. In some pixels formal values of abundance are higher than 100 vol.%. This can be ignored as artifacts. Since no significant olivine regions are located in the immediate surroundings of the peaks, intensive material transfer after the crater formation is unlikely to have occurred here.

The olivine spots on the northern wall are dark and appear as flow-like structures, containing up to 30 vol.% olivine. Their low albedo is unusual for such a mineral. It was assumed that their composition and structure is different than olivine peak has [9]. One may suppose that the recrystallized olivine grains are embedded in an opaque matrix of melted mafic-rich material.

Distinct olivine units with lower content (5–15 vol.%) are located on the crater floor to the west of the peaks. These exposures may be formed from the excavated materials simultaneously with the peaks, during crystallization of impact melt or composed from pre-impact olivine-contained rocks. Their composition has not been distinguished unambiguously. Spectral studies of the 1 μm absorption band have shown that the material of these areas may be composed of olivine as well as melted glasses [9, 10].

To solve this problem, we additionally applied our method to a well-known region containing glasses. This is the area of lunar pyroclastic deposits (LPD) in Mare Vaporum. Although the origin and composition of glasses are quite different, their spectral properties in the context of the absorption bands' positions and shapes are generally the same. The olivine is absent on this LPD formation according to our prediction. This enforces the confidence of olivine presence on the crater floor and high effectiveness of the proposed method to olivine sensing.

We consider the high olivine abundance on the northern wall upper cliffs as artifacts caused by photometry reduction shortcomings and/or improper application of the spectral mixing formula to fresh surfaces depleted with regolith.

Conclusion: We here offer a method to assess olivine abundance using the IBDs' ratio. Our results are consistent with [9], confirming three main types of olivine-bearing regions in crater Copernicus: (1) both central peaks (40-100 vol.%); (2) some olivine deposits on the crater floor (15 vol.%); (3) low-albedo spots and flows on the lower part of the northern wall (up to 30 vol.%). The proposed method shows high sensitivity to olivine content.

References: [1] Snyder G.A., et al. (1992) *Geochim. Cosmochim. Acta* 56, 3809-3823. [2] Pieters C., et al. (1982) *Science* 215, 59-61. [3] Lucey P., et al. (1986) *J. Geophys. Res.* 91, D344-D354. [4] Pinet P., et al. (1993) *Science* 260, 797-801. [5] Lucey P., et al. (2004) *J. Geophys. Res*. 31, L08701. [6] Tompkins S., et al. (1999) *Meteorite. Planet. Sci.* 34, 25-41. [7] Yamamoto S., et al. (2012) *Icarus* 218(1), 331-334. [8] Isaacson P., et al. (2011) *J. Geophys. Res.* 116, E00G11. [9] Dhingra D., et al. (2015) *Earth and Planet. Sci. Lett.* 420, 95-101. [10] Horgan B., et al. (2014) *Icarus* 234, 132-154. [11] Arnold J., et al. (2016) *J. Geophys. Res. Planets* 121, 1342-1361. [12] Surkov Y., et al. (2021) *Icarus* 355, 114123. [13] Shkuratov Y., et al. (2011) *Planet. Space Sci.* 59, 1326-1371. [14] Isaacson P., et al. (2011) *Meteorit. Planet. Sci.* 46, 228-251. [15] Johnson P. & Christy R. (1974) *Phys. Rev. B* 9, 5056-5070. [16] Shkuratov Y., et al. (2019) *Icarus* 321, 34-49. [17] Surkov Y., et al. (2020) *Icarus* 341, 113661.